

AFOSR-TR. 85-1056

2



TEXAS A&M UNIVERSITY
College Station, Texas

20000 801200

NONLINEAR DYNAMIC RESPONSE
OF
COMPOSITE ROTOR BLADES

Annual Letter

Prepared by

Dr. John J. Engblom
and
Dr. Ozden O. Ochoa

of the

Mechanical Engineering Department
Texas A&M University

Submitted to the

Air Force Office of Scientific Research
United States Air Force

Approved for public release;
distribution unlimited.

ME 4786-83-10

Contract No. F49620-82-K-0032
October 1983

Reproduced From
Best Available Copy

85 12 6 027

DTIC FILE COPY

AD-A162 158



NONLINEAR DYNAMIC RESPONSE
OF
COMPOSITE ROTOR BLADES

Annual Letter

Prepared by

Dr. John J. Engblom
and
Dr. Ozden O. Ochoa

of the

Mechanical Engineering Department
Texas A&M University

Submitted to the

Air Force Office of Scientific Research
United States Air Force

ME 4786-83-10

Contract No. F49620-82-K-0032
October 1983

AIR FORCE OFFICE OF SCIENTIFIC RESEARCH
MONITORING
THIS
DISTRICT
MATCHED
Chief, Technical Information Division

UNCLASSIFIED

SECURITY CLASSIFICATION OF THIS PAGE (When Data Entered)

| REPORT DOCUMENTATION PAGE | | READ INSTRUCTIONS BEFORE COMPLETING FORM |
|---|---|---|
| 1. REPORT NUMBER AFOSR-TR-83-1056 | 12. GOVT ACCESSION NO. <i>AD A163 158</i> | 3. RECIPIENT'S CATALOG NUMBER |
| 4. TITLE (and Subtitle) Nonlinear Dynamic Response of Composite Rotor Blades | 5. TYPE OF REPORT & PERIOD COVERED Interim Annual Report 1 Sept 1982 - 31 Aug 1983 | |
| 7. AUTHOR(s) John J. Engblom, Ozden O. Ochoa | 6. PERFORMING ORG. REPORT NUMBER ME 4785-83-10 | |
| 9. PERFORMING ORGANIZATION NAME AND ADDRESS Texas A&M University Mechanical Engineering Department College Station, TX 77843 | 8. CONTRACT OR GRANT NUMBER(s) F49620-82-K-0032 | |
| 11. CONTROLLING OFFICE NAME AND ADDRESS Air Force Office of Scientific Research/NA Building 410 Bolling AFB, DC 20332 | 10. PROGRAM ELEMENT, PROJECT, TASK AREA & WORK UNIT NUMBERS <i>61102 - 2307/B1 DAB</i> | |
| 14. MONITORING AGENCY NAME & ADDRESS (if different from Controlling Office) | 12. REPORT DATE October 1983 | |
| | 13. NUMBER OF PAGES 37 plus Appendices | |
| | 15. SECURITY CLASS. (of this report) Unclassified | |
| 15a. DECLASSIFICATION/DOWNGRADING SCHEDULE | | |
| 16. DISTRIBUTION STATEMENT (of this Report) Approved for Public Release, Distribution Unlimited | | |
| 17. DISTRIBUTION STATEMENT (of the abstract entered in Block 20, if different from Report) | | |
| 18. SUPPLEMENTARY NOTES | | |
| 19. KEY WORDS (Continue on reverse side if necessary and identify by block number) <div style="display: flex; justify-content: space-between;"> <div> <p>Composite Materials</p> <p>Nonlinear Dynamic Response</p> <p>Damage Mechanisms</p> <p>Finite Elements</p> <p>Large Displacement Formulation</p> </div> <div> <p>Interlaminar Shear and Normal Stresses</p> <p>Assumed Displacement and Hybrid Models</p> <p><i>Fundamental to the analysis of</i></p> </div> </div> | | |
| 20. ABSTRACT (Continue on reverse side if necessary and identify by block number) <p>Summarized are research activities related to Nonlinear Dynamic Response of Composite Rotor Blades. Fundamental to the analysis is the development of a continuum formulation that can accurately account for the effects of interlaminar shear and interlaminar normal stress variation thru-the-thickness of a laminate. Technical highlights of the research efforts to date are presented for each of the proposed tasks; namely, Nonlinear Displacement Formulation for Composite Media; Incorporate Damage Mechanisms into Dynamic Response Formulation and Correlation of Formulated Response Model with Experimental data. Also</p> | | |

20. included is a list of papers and abstracts submitted for publication/presentation as a result of the first year efforts.

UNCLASSIFIED

TABLE OF CONTENTS

| | |
|---|--------|
| I. Overview and Summary | Page 1 |
| II. Summary by Task | 2 |
| II.1. Task I: Nonlinear Displacement Formulation for Composite Media | 2 |
| II.1.1 Continuum Formulation | 2 |
| II.1.2 Large-Displacement Formulation | 5 |
| II.1.3 Computer Implementation | 7 |
| II.1.4 Analytical Verification | 10 |
| II.2. Task II: Incorporate Damage Mechanisms into Dynamic Response Formulation | 11 |
| II.3. Task III: Correlation of Formulated Response Model with Experimental Data | 13 |
| III. References | 14 |
| IV. Tables and Figures | 16 |
| V. Related Activities | 36 |
| VI. Appendices | |

| | |
|--------------------|-------------------------------------|
| Accession For | |
| NTIS CRA&I | <input checked="" type="checkbox"/> |
| DTIC TAB | <input type="checkbox"/> |
| Unannounced | <input type="checkbox"/> |
| Justification | |
| By | |
| Distribution/ | |
| Availability Codes | |
| Dist | Avail and/or Special |
| A-1 | |



I. OVERVIEW AND SUMMARY

Fundamental to this work is the development of a continuum formulation that can accurately account for the effects of interlaminar shear and interlaminar normal stress variation thru-the-thickness of a laminate. Furthermore, emphasis is particularly on tapered-twisted airfoil geometries which can be analytically represented as an assemblage of thin to moderately thick finite elements. To achieve solution efficiencies, the elements developed in this work are of the triangular/quadrilateral plate type as opposed to solid type elements.

On the basis of these requirements and considering viable alternatives, three suitable continuum formulations have been developed and incorporated within a finite element framework. These are herein denoted as the (i) Higher Order Displacement, (ii) Modified-Kirchhoff and (iii) Hybrid Stress formulations, respectively. A computer code has been developed to test the various elements on the basis of correlations with known analytical and numerical solutions. Linear small-displacement equations have been implemented in the code and many tests have been performed. It is noted that the code has some unique features, e.g., it can assemble elements having an unequal number of degrees of freedom at its nodes, it treats arbitrary ply orientations and it performs integration on a layer-by-layer basis through the laminate. Herein a layer refers to either a lamina or to a sub-set of laminae having equal ply orientations. The latter feature is essential in developing a fully nonlinear capability.

Significant efforts have also been devoted to developing a suitable large displacement formulation. Due to the requirement that interlaminar stresses be accurately represented, a total Lagrangian formulation is utilized and is based upon the complete Green's strain tensor. A geometric and large-displacement stiffness formulation has been implemented in the computer code based upon a form of the nonlinear strain-nodal displacement relationships suitable for each of the elements under development.

An extensive literature survey has been performed to identify analytically tractable methods of treating damage accumulation in composites. Since emphasis in this work is on the development of incremental response solutions, the computational approach must have the capability to (i) predict and

differentiate between relevant failure modes, (ii) modify constitutive equations appropriately and (iii) perform equilibrium iterations to assume stress redistribution based upon the extent of damage. Use of "piecewise smooth" failure criteria in conjunction with "damage state" variables provide a good basis for incrementally tracking damage. This approach is currently being formulated for incorporation in the computer code. Note that integration for an element is performed on a layer-by-layer basis which allows for damage effects to be characterized at the layer level.

Experimental data of the type required to substantiate damage predictions has been assembled to the extent possible. Analysis/test correlation efforts will be performed when the nonlinear formulation including damage effects is fully implemented. It is noted that useful experimental data is quite limited.

Technical progress in this program has been substantially on schedule. It is believed that the originally proposed three year program can be completed within the given time frame.

II. SUMMARY BY TASK

This section presents technical highlights of the research efforts to date for each of the three tasks. Details of the analytical formulation are presented in the Appendices.

II.1. TASK I: Nonlinear Displacement Formulation for Composite Media

II.1.1 Continuum Formulation

Two variational principles, the principle of Minimum Potential Energy and the Principle of Modified Complementary Energy, are used to develop two distinctly different finite element models, the assumed displacement model and the hybrid stress model respectively. These models incorporate the effects of transverse shear and normal deformations whose contributions are recognized as essential for accurate laminate analysis [1-6].

Within each formulation, element stiffness and force matrices are determined for each element, these matrices are then assembled to represent the final system of equations and a solution procedure for the unknown

nodal displacements are provided. Coordinate transformations to describe ply orientations of a composite media are taken into account. The in-plane stresses are calculated from constitutive relations of orthotropic continuum whereas transverse shear and normal stresses are calculated from equilibrium considerations.

The developed elements are tested for linear static and dynamic analysis. The test problems and the results are presented in Section II.1.4. The finite element models are herein briefly discussed.

i. Assumed Displacement Model

A. Higher Order Displacement Formulation

The thru-the-thickness effects can be incorporated into an analysis by choosing a displacement field that eliminates two major shortcomings of the classical plate theory; namely normals remain normal and in-plane displacements are linear thru the thickness. These shortcomings are eliminated by prescribing independently the reference surface displacements and rotations of the normal and including higher order terms for in-plane displacements. This is accomplished by the following variation

$$u(x,y,z) = u_0(x,y) + z\phi_x(x,y) + z^2\psi_x(x,y)$$

$$v(x,y,z) = v_0(x,y) + z\psi_y(x,y) + z^2\phi_y(x,y)$$

$$w(x,y,z) = w_0(x,y)$$

The neutral surface displacements are represented by u_0 , v_0 and w_0 , the rotation about y-axis is denoted by ψ_x and the rotation about the x-axis is ψ_y . The coefficients of z^2 , i.e., ϕ_x and ϕ_y , are contributions from transverse deformations [5,6].

The elements developed are designated as the quadrilateral higher order displacement (QHD) models. QHD40 is an eight-noded element with seven degrees of freedom (three midsurface displacements, two rotations and two higher order terms for in-plane displacements) per corner node and three degrees of freedom (transverse midsurface displacement and two rotations) per mid-side node. Element QHD28 is a simplified version of

QHD40 where the mid-side nodes are eliminated. It should be noted that when the two higher order terms for in-plane displacements at each corner node are omitted, QHD28 reduces to the widely used four-noded bilinear plate element (QHD20).

The transverse shear and normal stresses of QHD40 display a cubic variation thru-the-thickness. The displacement field, nodal degrees of freedom and the resulting stress fields are stated in Appendix IA.

B. Modified-Kirchhoff Formulation

The Kirchhoff-Love assumption for normals to the reference surface is relaxed by incorporating shear rotations as additional degrees of freedom in the formulation [9]. Thus the assumed displacement field allows the transverse shear deformations but neglects the transverse normal deformations. The rotations γ_x and γ_y are incorporated in the displacement variation as follows.

$$w(x,y) = w_0(x,y)$$

$$u(x,y,z) = u_0(x,y) - z\left(\frac{\partial w}{\partial x} + \gamma_x\right)$$

$$v(x,y,z) = v_0(x,y) - z\left(\frac{\partial w}{\partial y} + \gamma_y\right)$$

The transverse displacement $w(x,y)$ is chosen such that it will guarantee plausible stress fields which will characterize the transverse effects accurately.

This approach is implemented in the formulation of an eight-node quadrilateral element with 32 degrees of freedom - QD32, a six-node triangular element with 27 d.o.f. - TD27 and a seven-node triangular element with 27 d.o.f. - TD27M. The stress fields obtained for these elements represents a quadratic thru the thickness variation for the transverse shear stresses and a cubic variation for the transverse normal stress. The respective displacement fields, nodal degrees of freedom and stress fields are given in Appendix IB.

ii. Hybrid Stress Model

In this formulation a stress distribution within the interior of the element is expressed in terms of finite parameters such that equilibrium

is satisfied, also an assumed displacement distribution is used on the boundary of the element expressed in terms of generalized nodal displacements such that the interelement compatibility is retained [4].

The element developed, QHS32, is a four-node quadrilateral with 32 degrees of freedom. In addition to an assumed displacement field it has a 26-parameter stress field which provides cubic variation for transverse shear stresses and a quartic variation for transverse normal stress through the thickness of the laminate. The stress field along with the assumed displacement variation is stated in Appendix II.

II.1.2. Large Displacement Formulation

Inclusion of geometrically nonlinear effects in the formulation must be based upon both the geometry to be analyzed and upon the type of stress prediction capabilities desired. The classical approach to thin plate analysis has been to use the Kirchhoff-Love assumptions in conjunction with the nonlinear von Karman relations [11,12]. As previously indicated, the Kirchhoff-Love assumptions are relaxed in this work to allow for a more accurate definition of interlaminar-shear and interlaminar-normal stress variations. These stresses can vary substantially through-the-thickness for the geometries of interest, i.e., thin to moderately thick plate type structures. Furthermore, the requirement that these stresses be accurately determined means that the nonlinear portion of the strain-displacement relationship must contain all significant coordinate displacements. The complete Green's strain tensor is utilized in this work, therefore, to account for all significant contributions to the interlaminar stress field. With respect to fixed Cartesian coordinates x , y , and z , the strain tensor has the form

$$\epsilon_x = \frac{\partial u}{\partial x} + \frac{1}{2} \left[\left(\frac{\partial u}{\partial x} \right)^2 + \left(\frac{\partial v}{\partial x} \right)^2 + \left(\frac{\partial w}{\partial x} \right)^2 \right]$$

$$\gamma_{xy} = \frac{\partial u}{\partial y} + \frac{\partial v}{\partial x} + \left[\frac{\partial u}{\partial x} \frac{\partial u}{\partial y} + \frac{\partial v}{\partial x} \frac{\partial v}{\partial y} + \frac{\partial w}{\partial x} \frac{\partial w}{\partial y} \right]$$

where u , v and w represent displacements in the x, y, z coordinate directions, respectively. Note that the other strain components are obtained by a

suitable permutation. In small-displacement analysis, the quadratic terms are neglected to give simply the linear strain approximation.

Based on the Green's strain tensor, the strain to nodal point displacement relationship can be specified for elements under development. It takes the form

$$\{\epsilon\} = [B]\{\Delta\}$$

where $\{\epsilon\}$ is the vector of strain components, $\{\Delta\}$ the vector of nodal point displacements and $[B]$ a function of derivatives of the element shape functions. The quadratic terms in the strain tensor result in $[B]$ being a function of displacement state and, therefore, an incremental equilibrium formulation is required. The incremental strain-nodal displacement relationship takes the form

$$\{\delta\epsilon\} = ([B_0] + [B_L]) \{\delta\Delta\}$$

where $\{\delta\epsilon\}$ and $\{\delta\Delta\}$ represent incremental strains and nodal displacements, respectively, $[B_0]$ and $[B_L]$ are the small and large displacement contributions to the incremental strains. Based on the incremental equilibrium equations, the displacement formulation gives the force-displacement relationships

$$[K_0] = \int_V [B_0]^T [D] [B_0] dV$$

$$[K_L] = \int_V ([B_0]^T [D] [B_L] + [B_L]^T [D] [B_L] + [B_L]^T [D] [B_0]) dV$$

where $[D]$ is an elasticity matrix obtained simply from the constitutive equations and integration is over the volume V of the element. $[K_0]$ is denoted the small-displacement stiffness matrix and $[K_L]$ is denoted the large-displacement stiffness matrix. Since response is also a function of stress state, the geometrical stiffness matrix $[K_G]$ is required and is obtained from

$$[K_G]\{\delta\Delta\} = \int_V \epsilon [B_L]^T \{\sigma\} dV$$

where $\{\sigma\}$ is the vector of stress components. Note that the hybrid stress formulation similarly gives force-displacement forms involving the stress and displacement state.

Inertial effects are analytically treated as a mass matrix $[M]$ which is a function of density and the element shape functions (see Appendix III). These matrix forms are required in formulating static/dynamic response solutions and the incremental equilibrium equations have the general form

$$[M]\{\delta\ddot{u}\} + ([K_O] + [K_L] + [K_G])\{\delta u\} = \{\delta F\}$$

where the mass and stiffness matrices represent an assembly of the elemental matrices previously discussed, $\{\delta u\}$ and $\{\delta\ddot{u}\}$ represent the incremental displacements and accelerations for the mathematical model and $\{\delta F\}$ represents the vector of incrementally applied forces.

In developing a geometrically nonlinear formulation, the effort is largely in defining the incremental strain-nodal displacement relationship. Having developed this relationship for a particular element, stiffness matrices are readily developed as the preceding equations indicate. These relationships are presented in Appendix IV. The form of these equations is the same for all elements.

II.1.3. Computer Implementation

A computer code has been developed for the purpose of implementing the various continuum formulations. At present, the code performs the following functions:

- (i) element stiffness matrix generation
- (ii) element mass matrix generation
- (iii) assembly of equilibrium equations
- (iv) decomposition and solution of equilibrium equations
- (v) fundamental frequency and mode shape calculation

A characteristic of the elements under development is that node points can have different numbers of degrees of freedom, i.e., typically mid-side nodes have fewer degrees of freedom than corner nodes. The code has been fashioned to handle this condition. All of the integration is performed on

a layer-by-layer basis thru the thickness of the laminate. This approach is fundamental to developing the capability to allow for inelastic material behavior and, ultimately, to the inclusion of damage mechanisms in the formulation.

Since solution of the equilibrium equations is a vital component in the overall solution strategy, it is appropriate to discuss the numerical methodology used in solving these equations. The intent is to obtain a higher ordered variation of the transverse shear and normal stresses (σ_{xz} , σ_{yz} , and σ_{zz}) than can be obtained via the equilibrium equations. The solution procedure can be thought of as described below. Assume that the in-plane stresses (σ_{xx} , σ_{yy} , and σ_{xy}) within each layer of a particular element have been determined at selected locations, i.e., through solution of the constitutive equations. In the code as presently written, these locations are specified as the element centroid and element nodal points. The equilibrium equations (in the absence of body forces) have the indicial form

$$\sigma_{ij,j} = 0$$

from which it follows that the thru-the-thickness shear stress variation can be written in numerical form for the i^{th} layer as

$$\Delta\sigma_{xz_i} = -(\sigma_{xx,x} + \sigma_{xy,y})_i \Delta Z_i$$

and

$$\Delta\sigma_{yz_i} = -(\sigma_{xy,x} + \sigma_{yy,y})_i \Delta Z_i$$

Here, the left-hand-side represents the change in stress from the lower to the upper surface of the i^{th} layer and ΔZ_i is the thickness of the i^{th} layer at a particular location. The derivatives with respect to x and y in the expressions above are readily computed; this is because in-plane stresses within a layer are related to element displacements through derivatives of element shape functions in conjunction with a material definition.

For an n layered laminate, n equations can be written in terms of both the unknown shear stresses at layer interfaces and the shear stresses at the laminate surfaces. Assuming the laminate has shear-free surfaces, the equations above give n equations in $n-1$ unknowns, so that, the equation set is over-determined. The equations have the matrix form below.

$$\begin{bmatrix} 1 & & & \\ -1 & 1 & & \\ & -1 & 1 & \\ & & & \ddots & \\ & & & & 1 & -1 \end{bmatrix} \begin{Bmatrix} \sigma_{xz_2} \\ \vdots \\ \sigma_{xz_n} \end{Bmatrix} = \begin{Bmatrix} I_{xz_1} \\ \vdots \\ I_{xz_n} \end{Bmatrix}$$

$n \times (n-1)$ $(n-1) \times 1$ $(n \times 1)$

where $I_{xz_i} = -(\sigma_{xx,x} + \sigma_{xy,y})_i \Delta Z_i$ and σ_{xz_j} represents the shear stress acting at the interface of the $j-1$ th and j th layer. A similar equation set is obtained by replacing σ_{xz_j} with σ_{yz_j} and I_{xz_i} with I_{yz_i} . These equations are solved by utilizing a least-squares orthonormalization procedure [13]. Due to the simplicity of the terms in the coefficient matrix, a concise closed-form solution is obtained. Having determined the transverse shear stresses, the transverse normal stress variation is determined through the numerical form of the third equilibrium equation for the i th layer.

$$\Delta \sigma_{zz_i} = -(\sigma_{xz,x} + \sigma_{yz,y})_i \Delta Z_i$$

As before, the left-hand-side represents the change in stress through the i th layer. Appropriate polynomial functions are utilized to describe the σ_{xz} and σ_{yz} in-plane variation. These functions are differentiated to obtain the right-hand-side of the equations above. Again the equation set is overdetermined because the normal tractions are known at the laminate surfaces. Solving for σ_{zz} proceeds, therefore, in identically the same

manner as discussed in calculating σ_{xz} and σ_{yz} . Parenthetically, inclusion of body forces at a later date can be accomplished with little difficulty.

II.1.4. Analytical Verification

An approach to the successful application of Higher Order Displacement type elements, i.e., for thin to moderately thick geometries, is to utilize reduced numerical integration where as this is not necessary for Modified-Kirchhoff Formulation. This approximation technique brings along the choice of implementing it overall or selectively to the strain energy components. For the QHD formulation, only the transverse shear components are integrated with reduced order. The integration order may affect the physical behavior of the element by introducing spurious zero energy modes. It is desirable to have only rigid body modes since there does not yet seem to be a generally accepted method of controlling the additional modes. For QHD40, 3x3 Gaussian quadrature along with the 2x2 quadrature for the transverse shear components is employed. QHD28 and QHD20 formulations are similarly integrated with 2x2 and 1x1 Gaussian quadratures. Manipulation of quadrature rules may result in undesirable element behavior. The presence of spurious zero energy modes in addition to the rigid body modes may detract from overall performance. A spectral(eigenvalue) test is conducted with and without full quadrature to observe the zero energy modes of the QHD elements. The quadrature order, the number of zero eigenvalues and the corresponding number of spurious zero energy modes for QHD40, QHD28 and QHD20 are listed in Table 1. The spurious modes of QHD28 are illustrated in Figure 1.

It is also noteworthy to observe the effect of reduced integration on the representation of the generalized forces. In order to illustrate the effect, the forces associated with the transverse displacement of a corner node are sketched in Figs. 2A and 2B for QHD28 with and without reduced integration respectively.

To demonstrate the performance of QHD40, QHD28 and QD32 in comparison to classical plate theory and elasticity solutions, the example problems of Table 2 are solved.

Example 1. Simply Supported Square Plate with Sinusoidal Load.

The results, given in Tables 3 and 4 are comparisons of the elasticity solution of Pagano to those calculated via the QHD40, QD32 formulations. Figures 3A-B and 4A-B display the transverse normal stress variation for QHD40 and QD32 respectively at the center and at a point on the edge of the plate respectively.

Example 2. Simply Supported Square Plate with Uniform Load.

The results presented in Figure 5 and Figure 6 display the difference between the QHD formulation and the classical plate theory. The bending stresses displayed in Figure 6 for QHD28 are in close agreement with those of QHD40 but the transverse shear stresses of Figure 5 present rather poor correlations. The transverse shear stresses and bending stress of QHD32 are as shown in Figures 7 and 8.

Example 3. Cylindrical Bending

The transverse shear stress, σ_{xz} , calculated via the QHD40 and QD32 formulations is illustrated in Figure 9 and 10 respectively. The bending stress σ_{xx} of QHD40 is displayed in Figure 11 and σ_{xx} of QD32 is shown in Figure 12. The results are compared to the elasticity solution obtained by Pagano.

Verification of the dynamics portion of the computer code has been limited thus far due to the emphasis placed on obtaining good statical results. A first check has been performed, however, in calculating the fundamental frequency of a simply supported (isotropic) plate. The calculated frequencies for elements QHD28, QHD40 and QD32 are all within 2% of the closed-form solution for a simple 36 element plate model.

II.2. TASK II: Incorporate Damage Mechanisms into Dynamic Response Formulation

The literature survey performed has been quite helpful in terms of delineating the viable approaches to including damage mechanisms in the analysis. Relevant failure modes of interest include those listed below.

- (i) fiber fracture
- (ii) fiber-matrix debonding
- (iii) matrix cracking (parallel and transverse to fibers)
- (iv) delamination

Several smooth failure criteria, e.g., [14-17] have been developed in recent years to represent the failure of composites. These criteria, to varying degrees, can predict "failure" but do not identify a particular mode of failure. In performing incremental "damage" analysis, it is essential to both predict failure and to characterize it, e.g., do fibers rupture, does delamination occur, etc. The computational approach must, therefore, differentiate between viable failure modes and appropriately alter the constitutive equations on an incremental basis. This can be accomplished by implementing a piecewise smooth failure criteria, e.g., [18] in the finite element formulation. The general failure criteria is then comprised of m separate inequalities of the form

$$F_j(\{\sigma\}) < 1 \quad ; \quad j = 1, 2, \dots, m$$

at each layer level within each element. These criteria can differentiate between (i) tensile and compressive fiber failure, (ii) tensile and compressive matrix failure and (iii) delamination at layer interfaces.

As progressive damage occurs throughout incremental loading (whether it be static or dynamic), it is essential that violation of failure criteria inequalities be reflected in modification of the material properties. This can be achieved by including damage state variables [19] in the constitutive equations to reflect "stiffness reduction." These equations can be represented as

$$\{\sigma\} = [D][\gamma]\{\epsilon\}$$

where $[D]$ represents the material matrix and $[\gamma]$ contains the damage state variables. The latter provide the basis for changing the D_{ij} terms based upon the extent to which the failure criteria are violated.

In conjunction with the above it is essential to perform equilibrium iterations within each analysis increment. This is required to assure that stress redistribution is properly accounted for as damage progresses. Currently the approach to modelling "damage mechanisms" is under development for implementation in the formulations.

II.3.3 TASK III: Correlation of Formulated Response Model with Experimental Data

Some quantitative data relating to the impact damage of composite specimens has been assembled [21-23]. It will be utilized along with any additional data obtained to perform analysis/test correlations. Since the nonlinear formulation including damage effects is not complete, no use of the test data has been made to this point. Much effort has been devoted, however, to correlating the analysis with both closed-form and numerical solutions as previously discussed.

III. REFERENCES

1. Whitney, J. M., "The Effects of Transverse Shear Deformation on the Bending of Laminated Plates," J. Composite Materials, 1969, Vol. 3, p. 534.
2. Pagano, N. J., "Stress Fields in Composite Laminates," Int. J. Solids and Structures, 1978, Vol. 14, p. 385-400.
3. Barker, R. M., Fu-Tien Lin, Dana, J. R., "Three Dimensional Finite Element Analysis of Laminated Composites," Computers & Structures, 1972, Vol. 2, p. 1013-1029.
4. Pian, T. H. H., and Tong, P., "Finite Element Methods in Continuum Mechanics," Advances in Applied Mechanics, 1972, Vol. 2, p. 1-58.
5. Reddy, J. N., "Bending of Laminated Anisotropic Shells by a Shear Deformable Finite Element," Fiber Science and Technology, 1982, Vol. 2, p. 9-24.
6. Pagano, N. J., "On the Calculation of Interlaminar Normal Stress in Composite Laminates," J. of Composite Materials, 1974, Vol. 8, p. 65-81.
7. Spilker, R. L., Chow, S. C. and Orringer, O., "Alternate Hybrid-Stress Elements for Analysis of Multilayer Composite Plates," J. Composite Materials, 1977, Vol. 11, p. 51-70.
8. Mau, S. T., Tong, P., and Pian, T. H. H., "Finite Element Solutions for Laminated Thick Plates," J. Composite Materials, 1972, Vol. 6, p. 304-305.
9. Pagano, N. J., "Exact Solutions for Composites Laminates in Cylindrical Bending," J. Composite Materials, 1969, Vol. 3, p. 398-411.
10. Pryor, C. W., and Barker, R. M., "Finite Element Analysis Including Transverse Shear Effects for Application to Laminated Plates," AIAA Journal, 1971, p. 912-917.
11. Whitney, J. M., and Leissa, A. W., "Analysis of Heterogeneous Anisotropic Plates," Journal of Applied Mechanics, 1969, Vol 36, p. 261-266.
12. Giri, J., and Simites, G. J., "Deflection Response of General Laminated Composite Plates to In-Plane and Transverse Loads," Fiber Science and Technology, 1980, Vol. 13, p. 225-242.
13. Whittaker, E. and Robinson, G., The Calculus of Observations, Blackie and Son, Limited, Glasgow, 1944.

14. Hill, R., "A Theory of the Yielding and Plastic Flow of Anisotropic Materials," Proceedings of the Royal Society, London, 1948, Series A, Vol. 193, p. 281-290.
15. Tsai, S.W., "Strength Characteristics of Composite Materials, NASA CR-224, 1965.
16. Hoffman, I., "The Brittle Strength of Orthotropic Materials," J. Composite Materials, 1967, Vol. 1, p. 200-206.
17. Tsai, S.W. and Wu, E.M., "A General Theory of Strength for Anisotropic Materials," J. Composite Materials, 1971, Vol. 5, p. 58-81.
18. Hasnin, Z., "Failure Criteria for Unidirectional Composites," J. Applied Mechanics, 1980, Vol. 47, p. 329-334.
19. Nuismer, R. J., ARO-NSF Research Workshop on Mechanics of Composite Materials, Duke Univ., 1978, p. 55-77.
20. Prewo, K. M., "Development of Impact Resistant Metal Matrix Composites," AFML-TR-75-216, 1975.
21. Novak, R. C., "Composite for Blade Development Resin Matrix Composites," United Technologies Report R76-214278-1, 1976.
22. Prewo, K. M., "Composite for Blade Development Metal Matrix Composites," United Technologies Report R76-214278-2, 1976.
23. Veltri, R. D., and Prewo, K. M., "The Slow Indention Testing of Simulated Blade Specimens," United Technologies Report, R77-216956-1, 1977.
24. Daniel, I. M. and Leber, T., "Wave Propagation in Fiber Composite Laminates," NASA-CR-135086, 1977.
25. Engblom, J. J., "Coupled Fluid/Structure Response Predictions for Soft Body Impact of Airfoil Configurations," ASME - Emerging Technologies in Aerospace Structures, Design, Structural Dynamics and Materials, 1980, p. 209-223.
26. Bertke, R. S., "Local Leading Edge Damage from Hand Particle and Soft Body Impacts (Task IV B)," AFWAL-TR-82-2044, 1982.
27. Bertke, R. S., "Structural Element and Real Blade Impact Testing," Univ. of Dayton Report UDRI-TR-82-02, 1982.
28. Storace, A. F., "Foreign Object Impact Design Criteria," General Electric Company Interim Report for Contract # F33615-77-C-5221, 1982.

IV. TABLES AND FIGURES

Table 1. Spurious Zero Energy Nodes of the QHD Family

| | Quadrature Order | Number of Zero Eigenvalues | Number of Spurious Modes |
|-------|---|----------------------------|--------------------------|
| QHD40 | 3x3 with 2x2 for transverse shear terms | 6 | 0 |
| QHD28 | 2x2 with 1x1 for transverse shear terms | 9 | 3 |
| QHD20 | 2x2 with 1x1 for transverse shear terms | 8 | 2 |

Table II. Geometric and Material Properties of the Example Problems

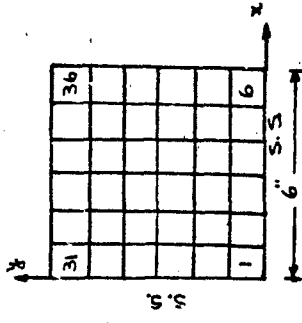
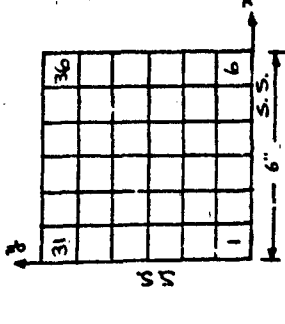
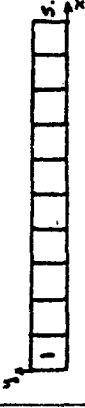
| | Example 1 | Example 2 | Example 3 |
|-----------------|---|--|---|
| Loading | Sinusoidal $q = 100 \sin \frac{\pi x}{a} \sin \frac{\pi y}{a}$ | Uniform $q = 100$ | Cylindrical Bending $q = 100 \sin \frac{\pi x}{a}$ |
| Material | Graphite/Epoxy | Graphite/Epoxy | Graphite/Epoxy |
| E_L/E_T | 25 | 40 | 25 |
| G_{LT}/G_{TT} | 2.5 | 1.2 | 2.5 |
| ν_{LT} | 0.25 | 0.25 | 0.25 |
| Aspect Ratio, S | 4, 10, 20 | 10 | 10 |
| Ply Orientation | $0^\circ/90^\circ/0^\circ$ | $0^\circ/90^\circ/90^\circ/0^\circ$ | $0^\circ/90^\circ/0^\circ$ |
| |  <p>Quadrant of a plate</p> |  <p>Quadrant of a plate</p> |  <p>Half a strip</p> |

Table III. Stress Field for Simply Supported Square Plate
with Sinusoidal Loading. $q = q_0 \sin \frac{m\pi x}{a} \frac{n\pi y}{a}$

| Aspect Ratio, S | $\sigma_x/q_0 s^2$ $(\frac{a}{2}, \frac{a}{2}, \pm \frac{h}{2})$ | | $\sigma_y/q_0 s^2$ $(\frac{a}{2}, \frac{a}{2}, \pm \frac{h}{6})$ | | $\sigma_{xy}/q_0 s^2$ $(0, 0, \pm \frac{h}{2})$ | | $\sigma_{xz}/q_0 s$ $(0, \frac{a}{2}, 0)$ | | $\sigma_{yz}/q_0 s$ $(\frac{a}{2}, 0, 0)$ | |
|-----------------|---|--------|---|--------|--|--------|--|--------|--|--------|
| | QHD40 | Elast. | QHD40 | Elast. | QHD40 | Elast. | QHD40 | Elast. | QHD40 | Elast. |
| 4 | 0.392 | 0.755 | 0.415 | 0.534 | 0.0425 | 0.0505 | 0.339 | 0.282 | .0962 | 0.2172 |
| 10 | 0.501 | 0.590 | 0.218 | 0.288 | 0.0265 | 0.0289 | 0.411 | 0.357 | .0541 | 0.1228 |
| 20 | 0.532 | .552 | 0.180 | 0.210 | .0222 | 0.0234 | 0.431 | 0.385 | .0423 | .0938 |

Table IV. Stress Field for Simply Supported Square Plate
with Sinusoidal Loading. $q = q_0 \sin \frac{\pi x}{a} \sin \frac{\pi y}{a}$

| | $\sigma_x/q_0 s^2$ $(\frac{a}{2}, \frac{a}{2}, \pm \frac{h}{2})$ | | $\sigma_y/q_0 s^2$ $(\frac{a}{2}, \frac{a}{2}, \pm \frac{h}{2})$ | | $\sigma_{xy}/q_0 s^2$ $(0, 0, \pm \frac{h}{2})$ | | $\sigma_{xz}/q_0 s$ $(0, \frac{a}{2}, 0)$ | | $\sigma_{yz}/q_0 s$ $(\frac{a}{2}, 0, \gamma)$ | |
|------------------------|---|--------|---|--------|--|--------|--|--------|---|--------|
| | QD32 | Elast. | QD32 | Elast. | QD32 | Elast. | QD32 | Elast. | QD32 | Elast. |
| Aspect Ratio, S | | | | | | | | | | |
| 4 | .395 | 0.755 | 0.519 | 0.534 | .044 | 0.0505 | 0.417 | 0.282 | 0.181 | 0.2172 |
| 10 | 0.503 | 0.590 | 0.247 | 0.288 | .027 | 0.0289 | 0.429 | 0.357 | .071 | 0.1228 |
| 20 | 0.534 | .552 | 0.170 | 0.210 | .022 | 0.0234 | 0.442 | 0.385 | .049 | .0938 |
| Classical Plate Theory | .545 | | 0.141 | | .022 | | .447 | | 0.041 | |

Figure 1. Spurious zero energy modes of QHD28

Figure 2. Generalized forces associated with the transverse displacement w_0 of a corner node with full quadrature as shown in (A) and with reduced integration as in (B) for QHD28.

Figures 3 & 4. Transverse normal stress, σ_{zz} , variation for QHD40 and QD32 respectively, at (A): center of the plate ($\bar{\sigma}_z = \bar{\sigma}_z/100$) and at (B): a point on the edge of the plate ($\bar{\sigma}_z = 10\sigma_z$).

Figures 5 & 6. Thru-the-thickness σ_{xz} variation in element #6. σ_{yz} variation in element #31; in comparison to CPT results ($\bar{\sigma}_{xz} = \bar{\sigma}_{xz}/100$, $\bar{\sigma}_{yz} = \bar{\sigma}_{yz}/100$) for QHD40 and QD32 respectively.

Figures 7 & 8. Comparison of bending stresses, of QHD40, QHD28, and QD32 to that of CPT in element #36. ($\bar{\sigma}_x = \bar{\sigma}_x/100$)

Figures 9 & 10. Transverse shear stress, σ_{xz} , for QHD40 & QD32 in comparison to elasticity solution of Pagano in element #20. ($\bar{\sigma}_{xz} = \bar{\sigma}_{xz}/100$)

Figures 11 & 12. Bending stress, σ_{xx} , variation of QHD40 and QD32 respectively in comparison to elasticity solution in element #1. ($\bar{\sigma}_x = \bar{\sigma}_x/100$)

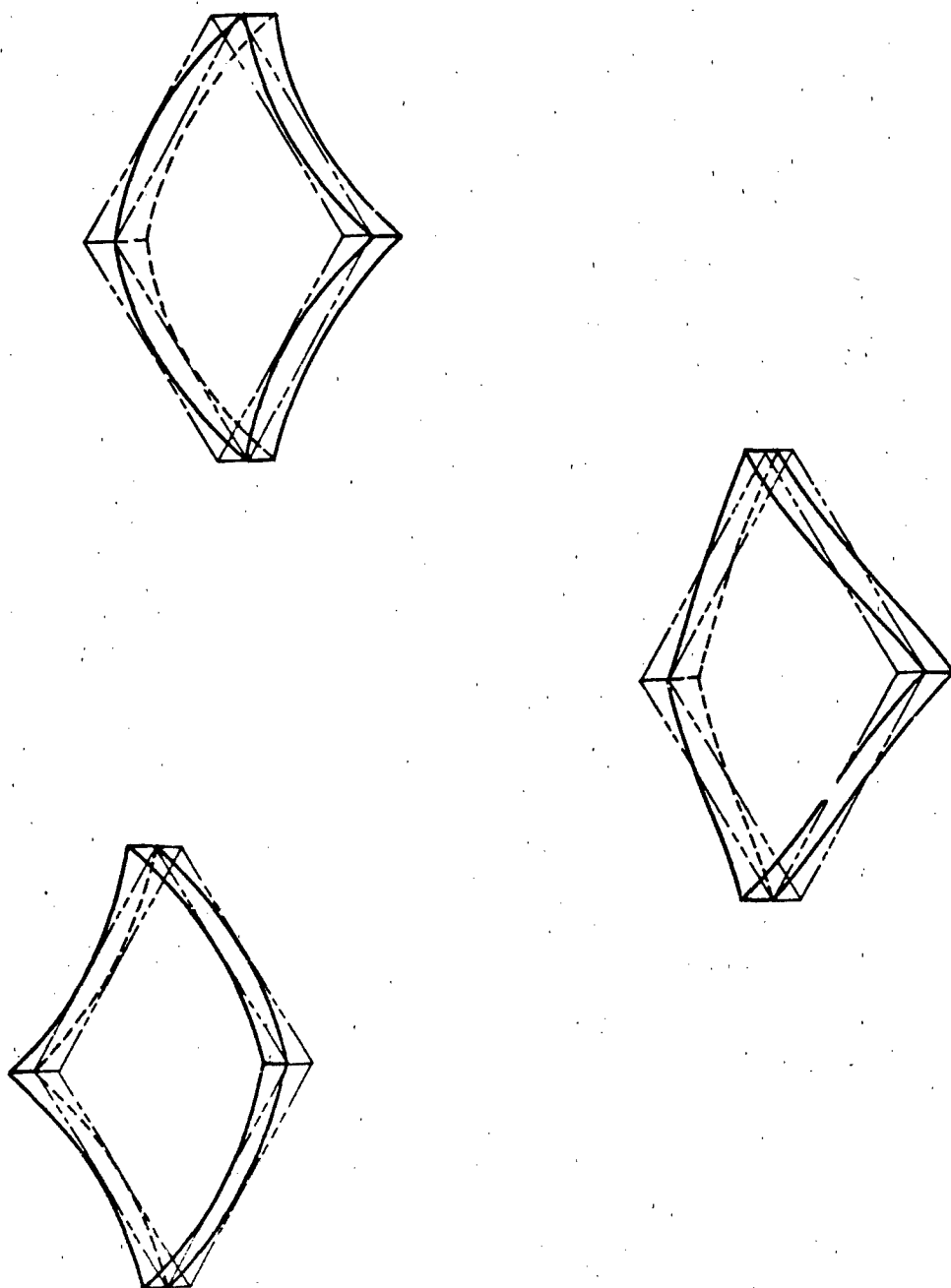


Fig. 1

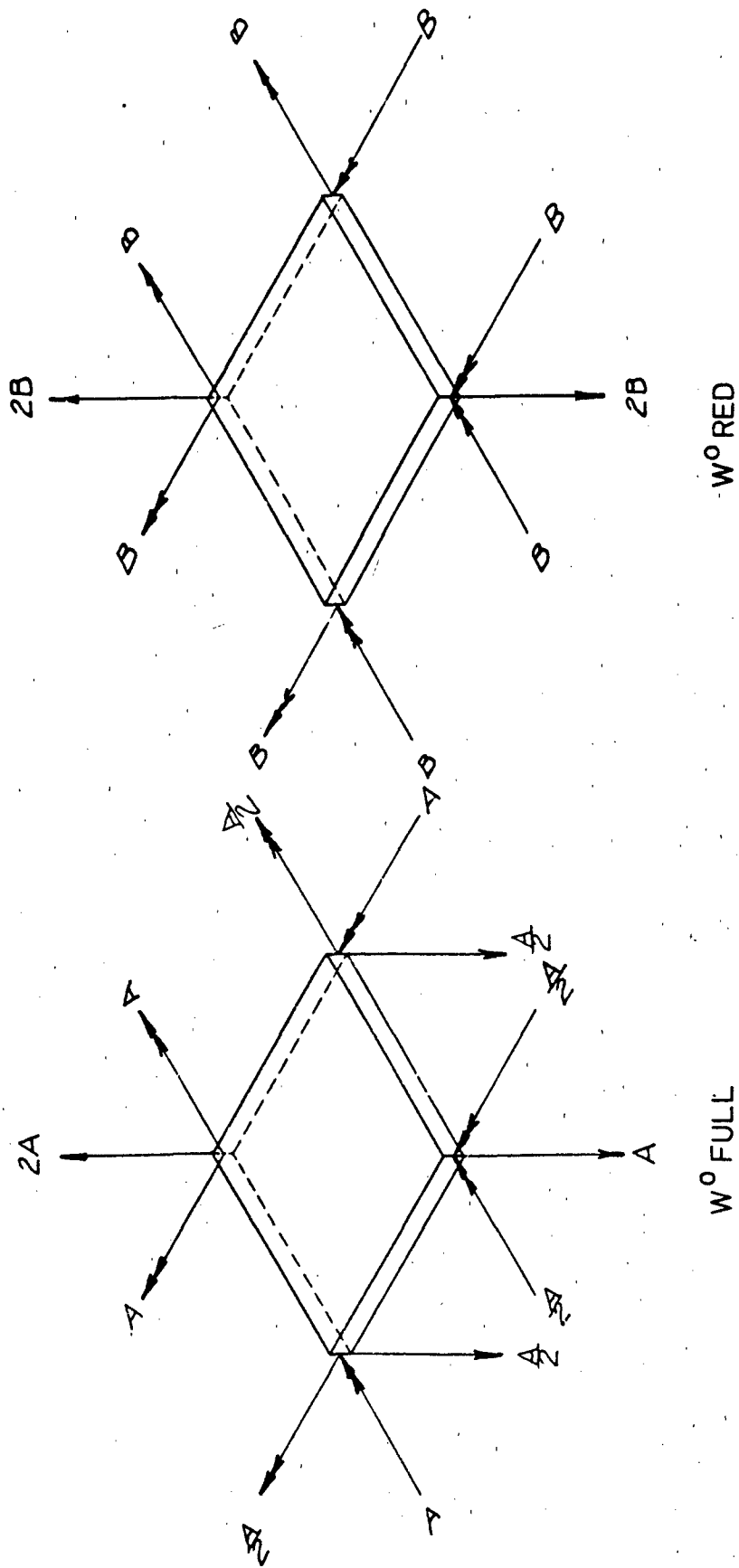


Fig. 2

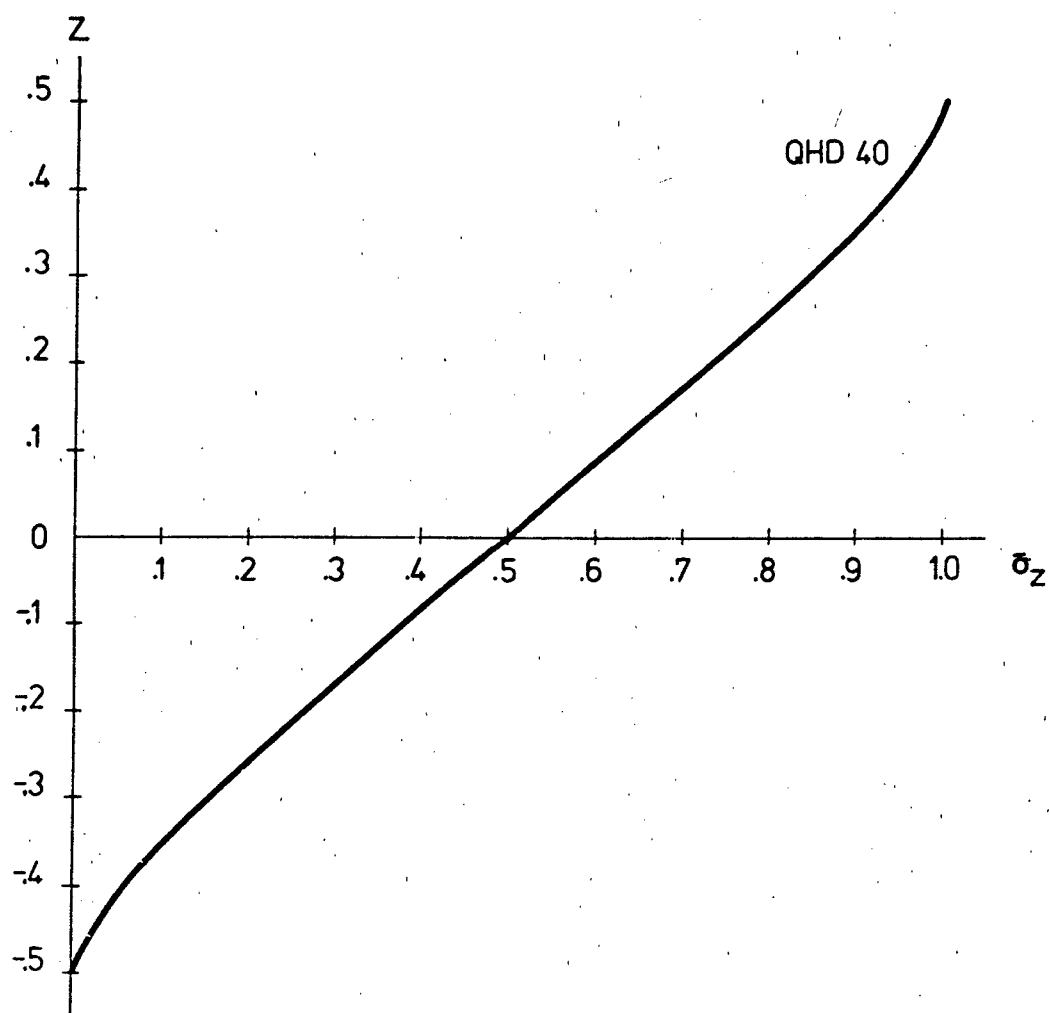


Fig. 3A

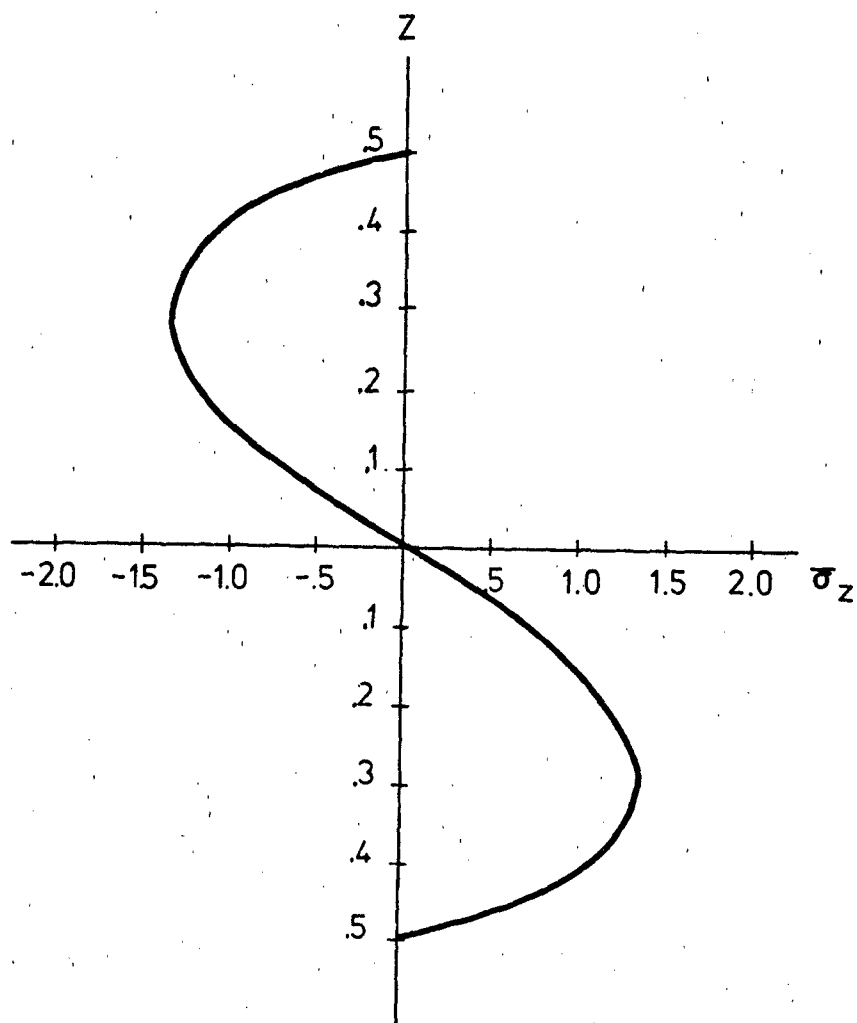


Fig. 3B

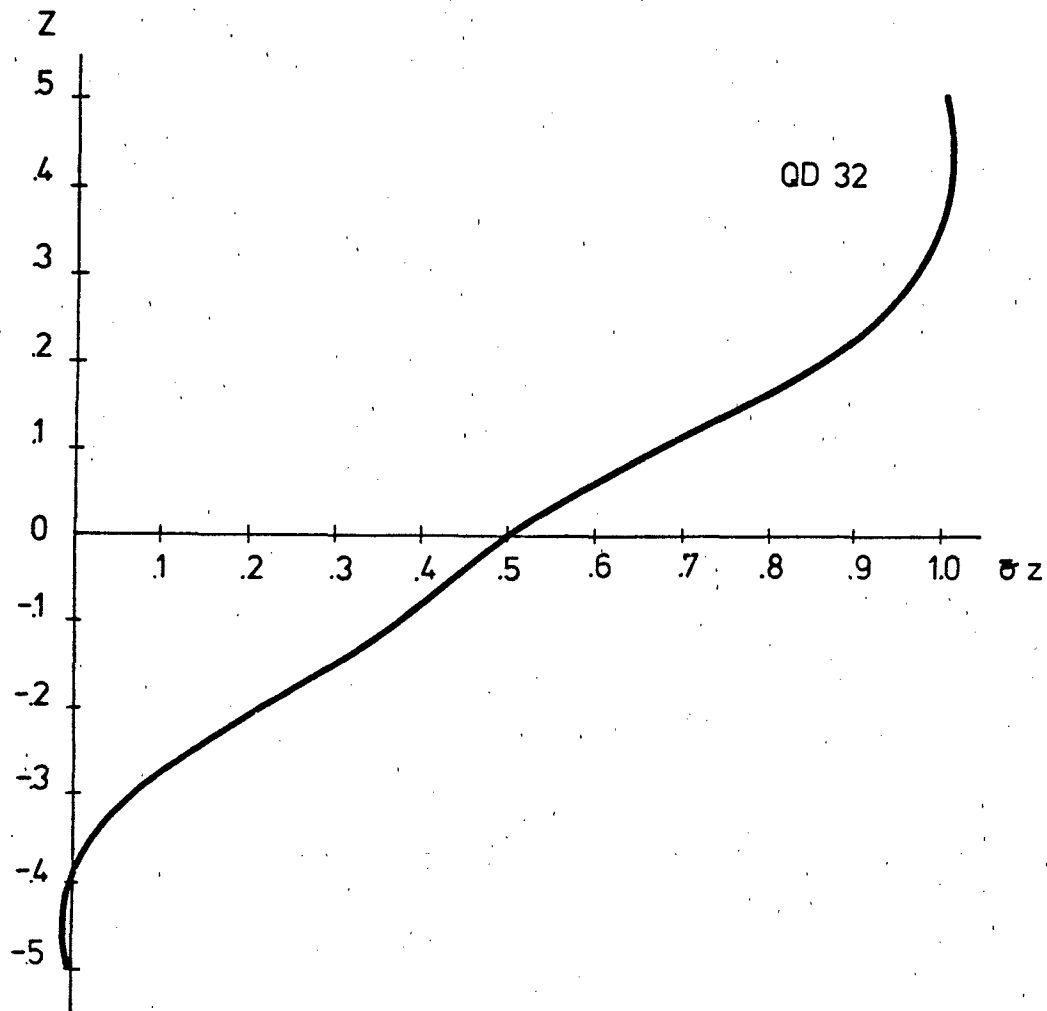


Fig. 4A

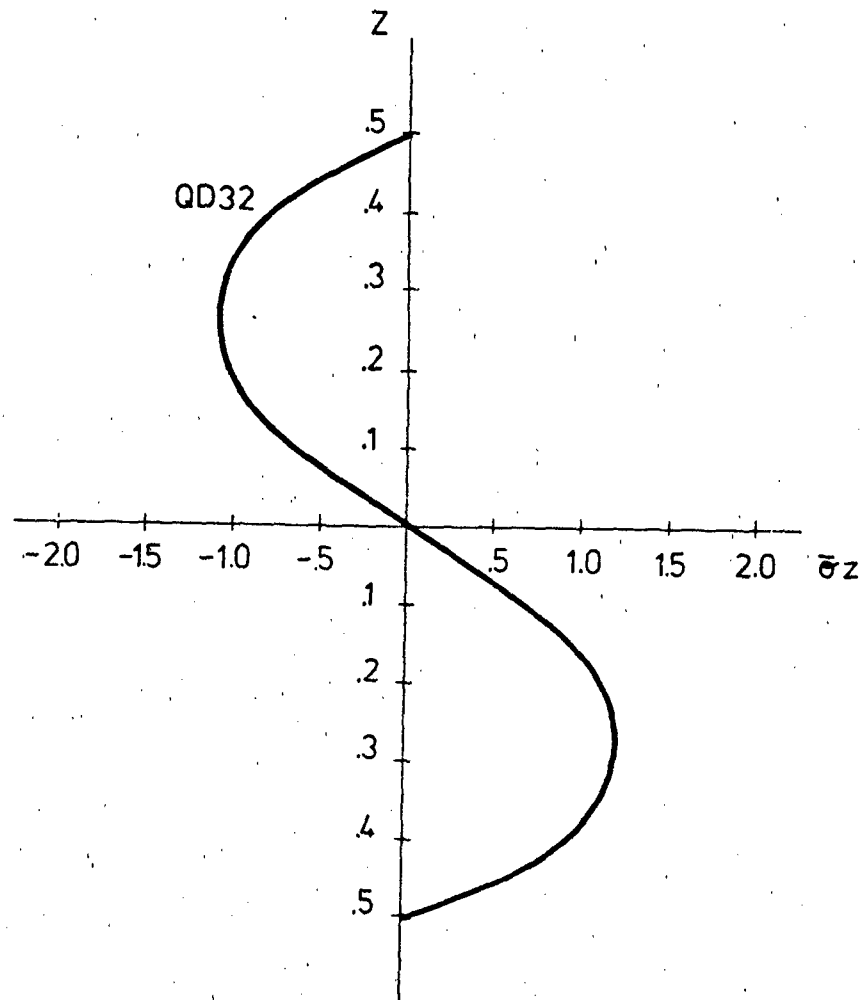


Fig. 4B

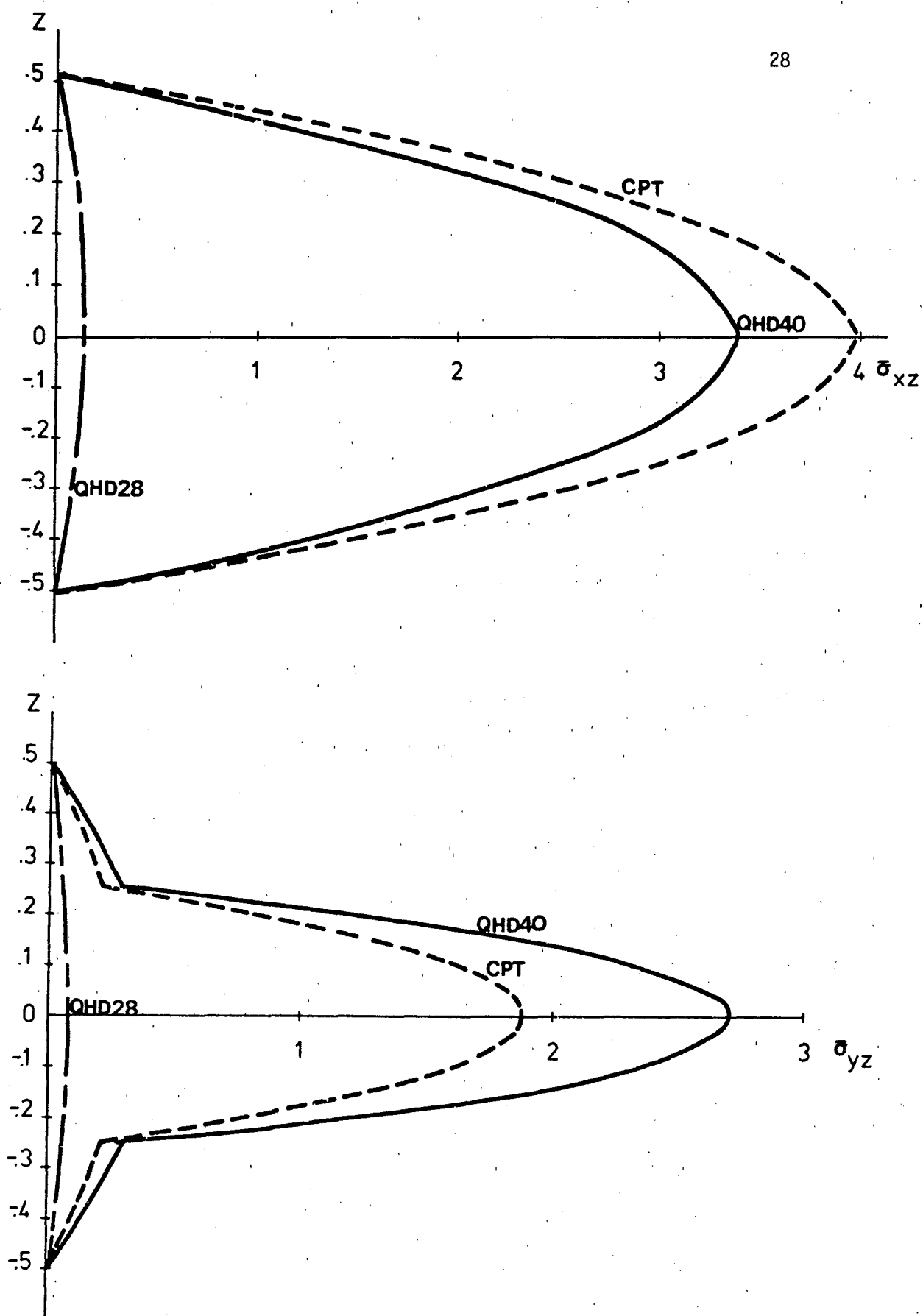


Fig. 5

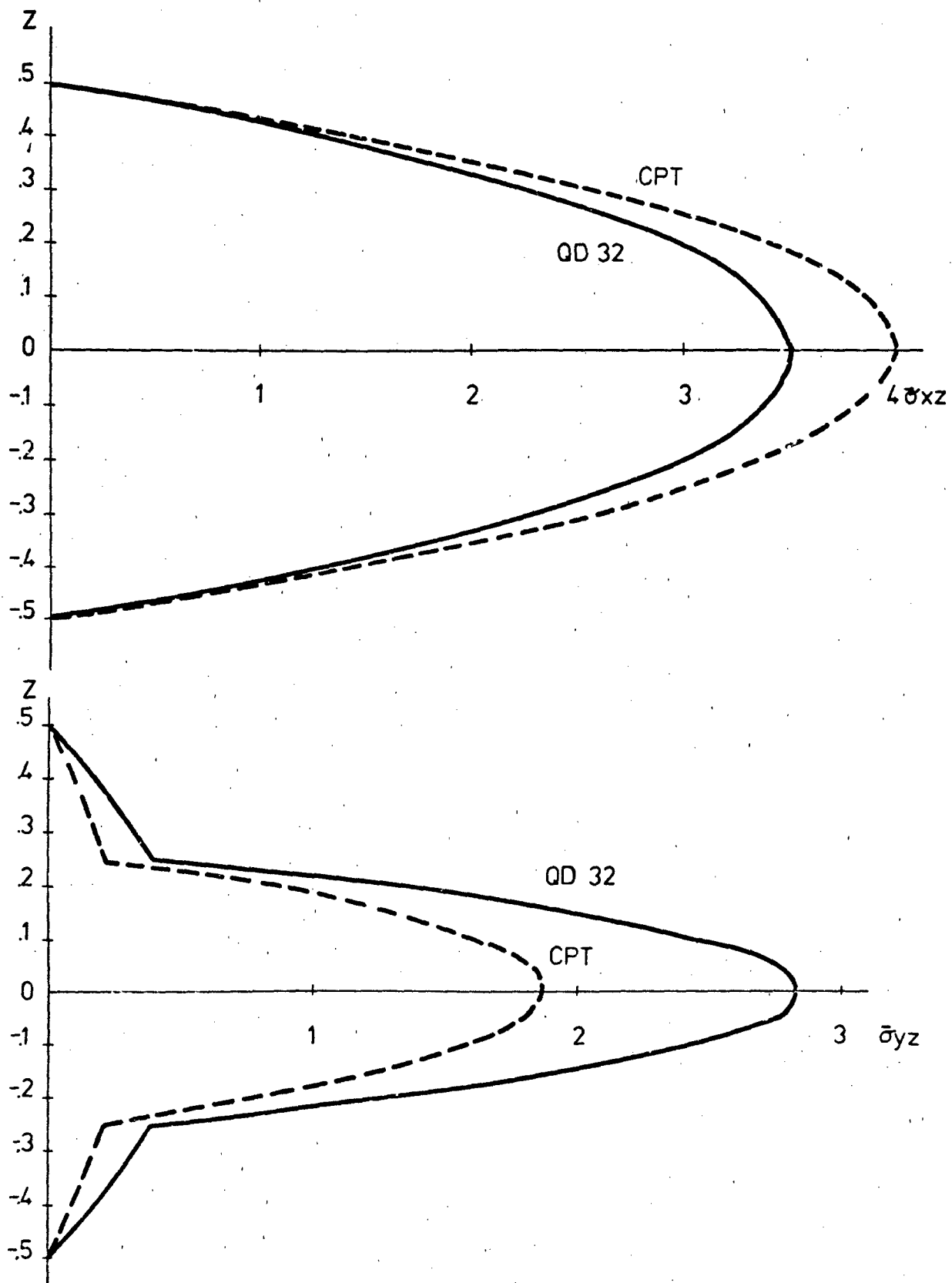


Fig. 6

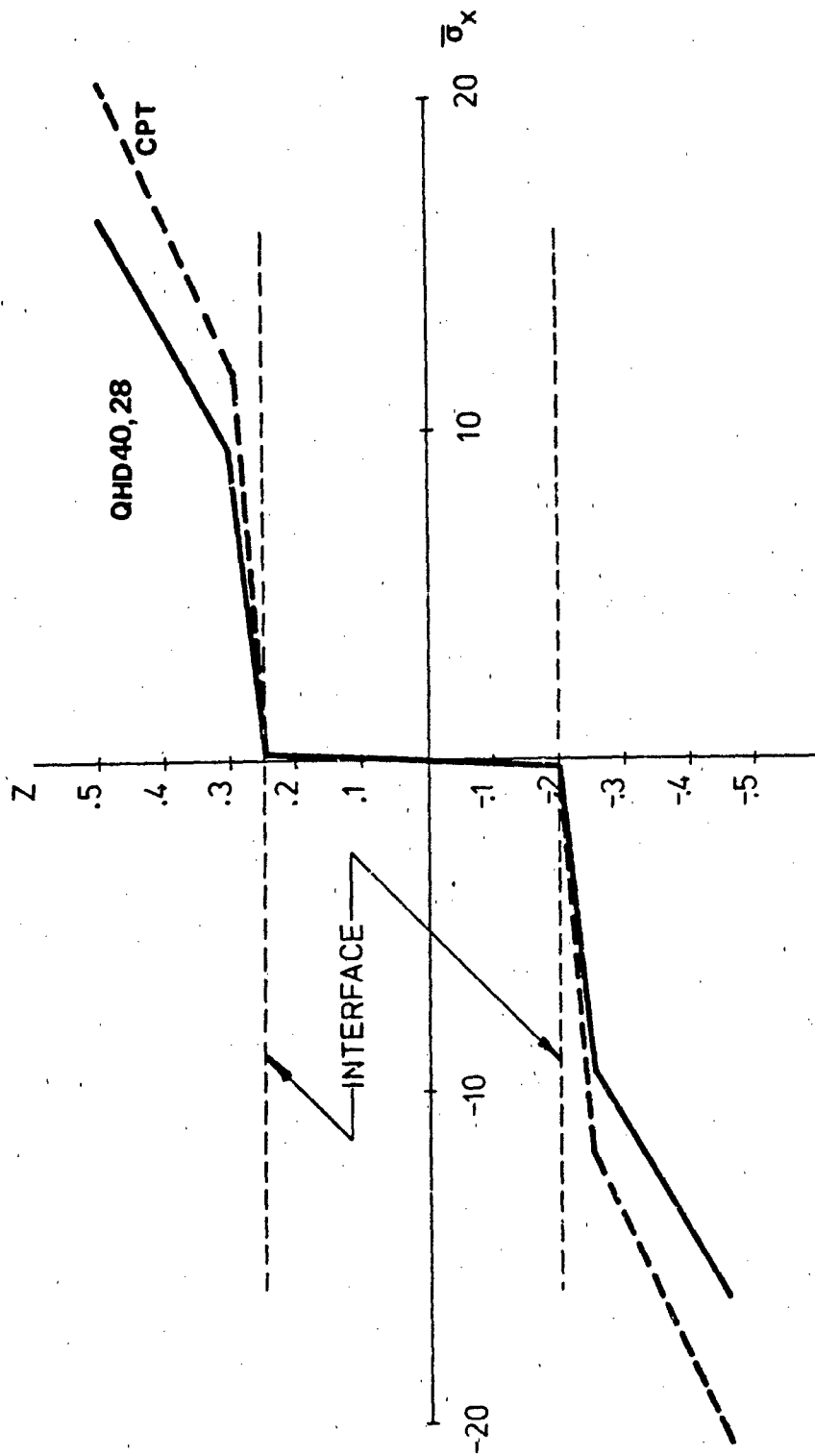


Fig. 7

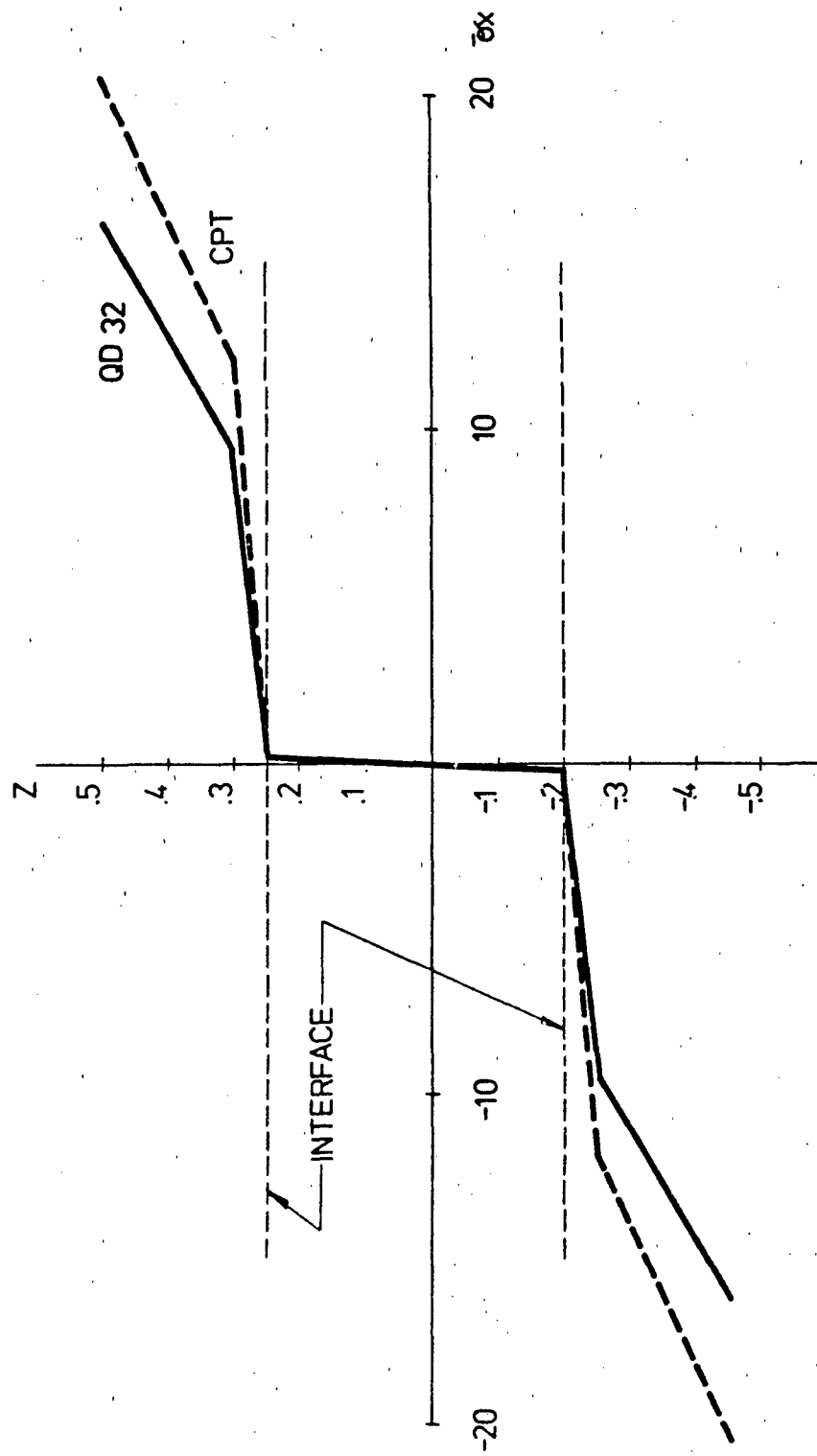


Fig. 8

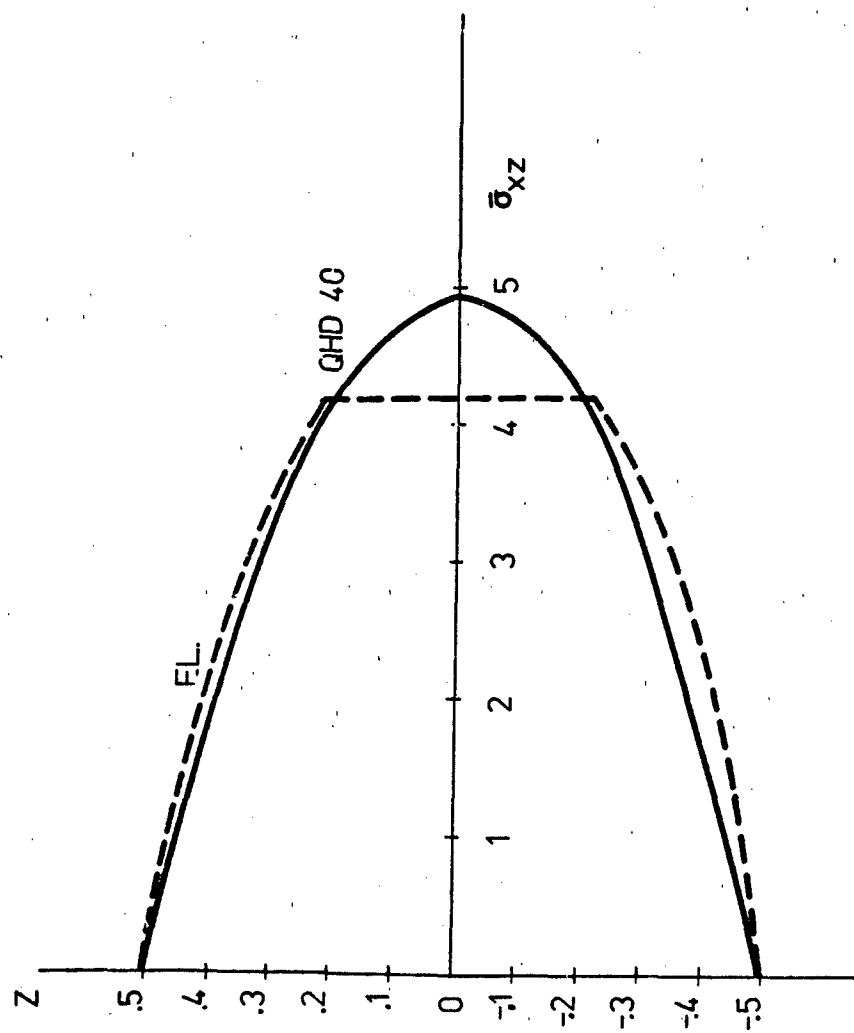


Fig. 9

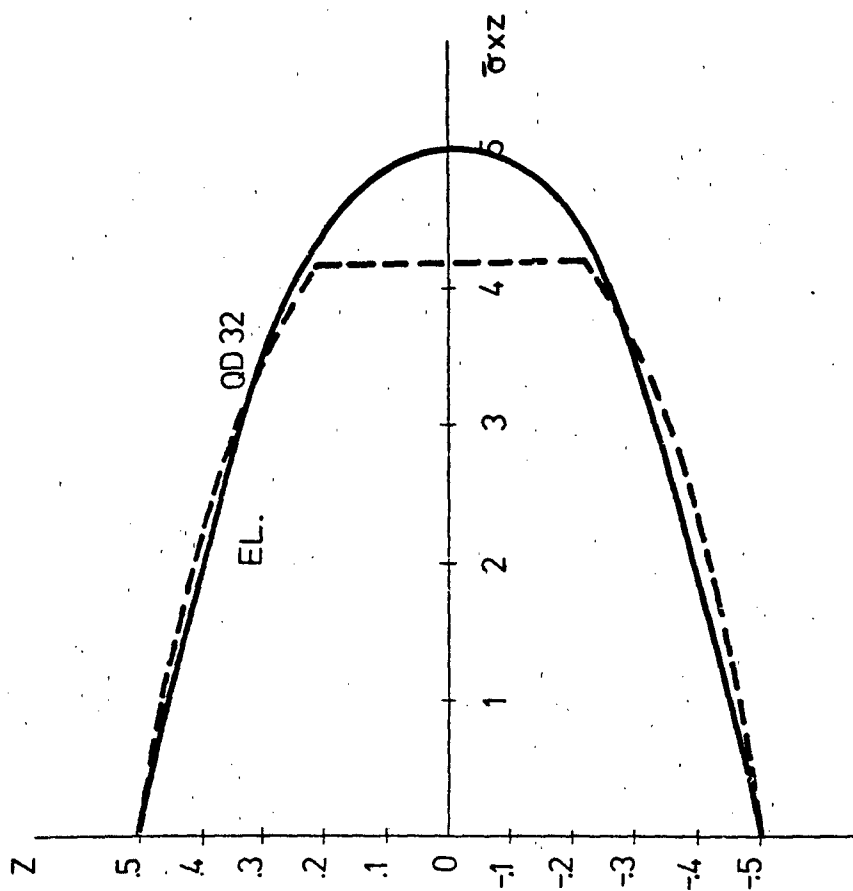


Fig. 10

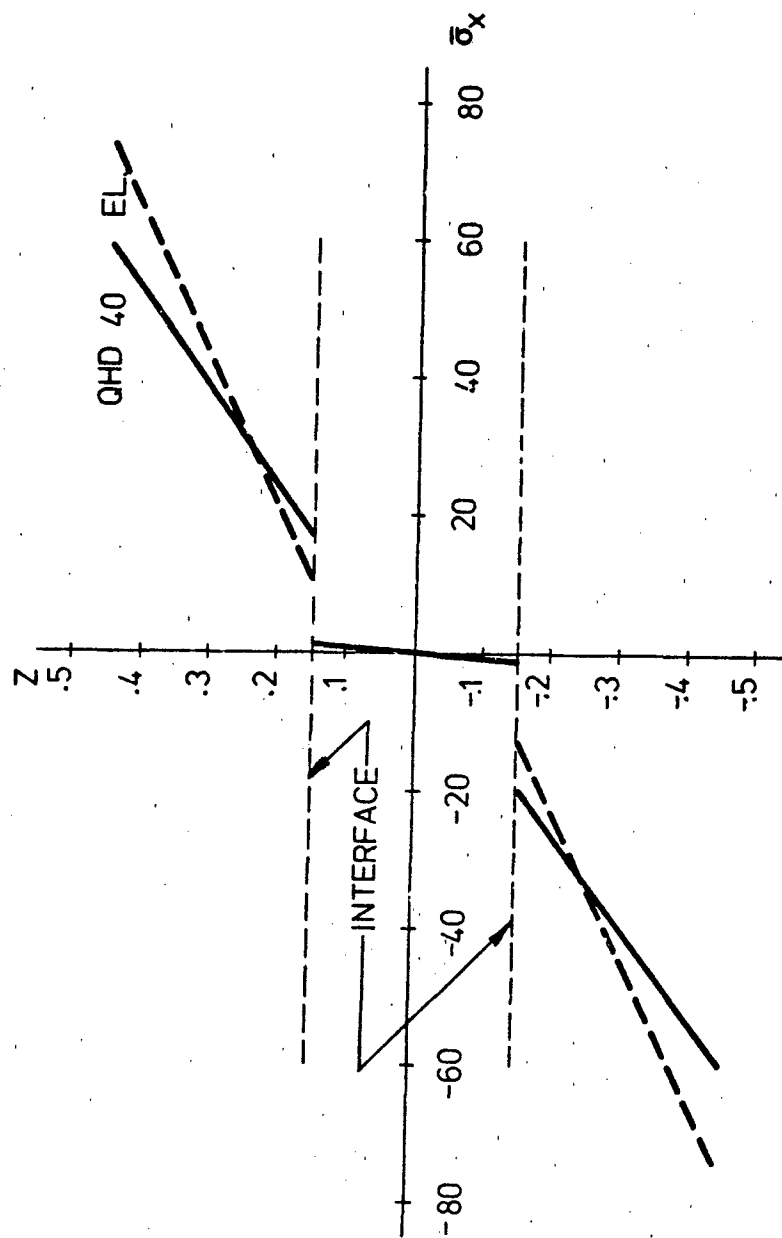


Fig. 11

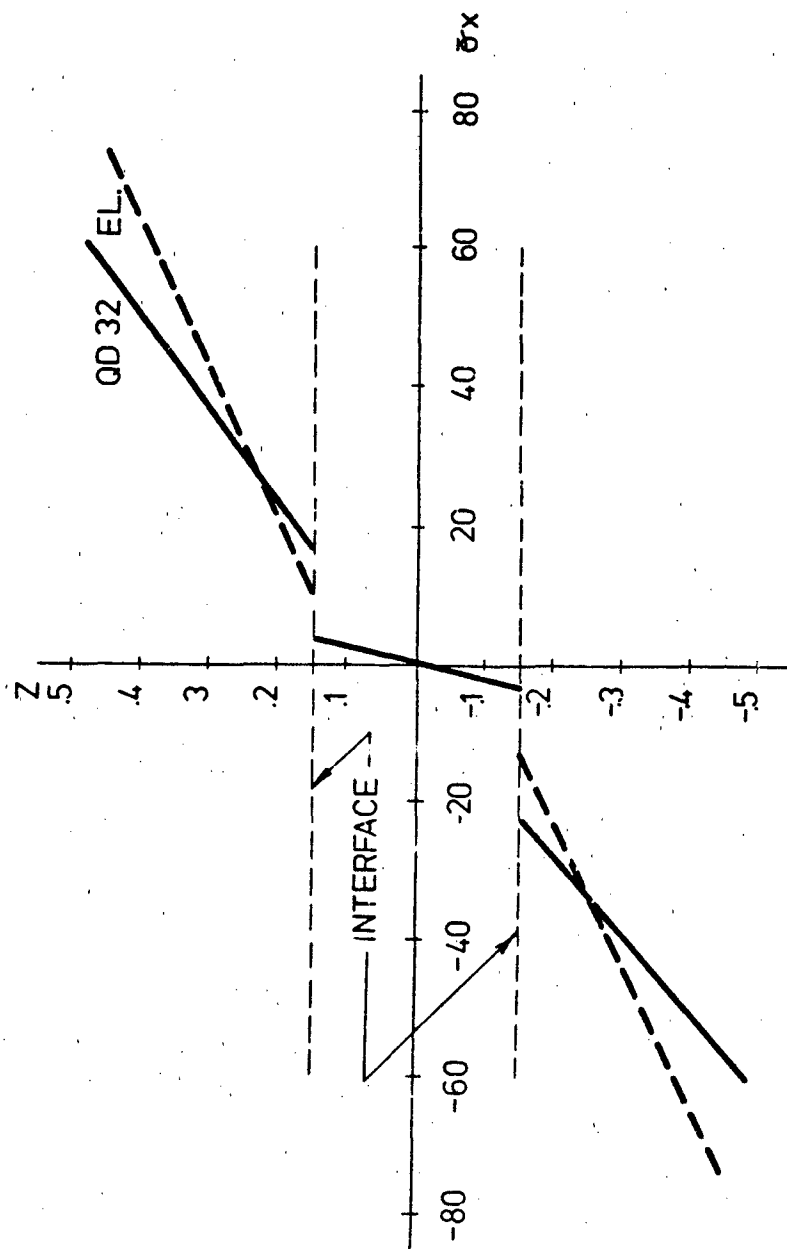


Fig. 12

V. RELATED ACTIVITIES

Following is a list of abstracts and papers that have been submitted for presentation/publication as a result of the present research efforts. (All co-authored by J.J. Engblom and O.O. Ochoa)

- Abstracts Submitted

25th Structures, Structural Dynamics and Materials Conference, Palm Springs, California, May 14-16, 1984

"Through-the-Thickness Stress Predictions for Advanced Composite Material Configurations"

Symposium on Advances and Trends in Structures and Dynamics, Washington, DC, October 22-25, 1984

"Interlaminar Stress Predictions for the Nonlinear Response of Composite Material Configurations"

and

"Inclusion of Damage Mechanisms in Finite Element Formulation of Composite Material Configurations"

- Papers Submitted

International Journal for Numerical Methods in Engineering

"Thru-the-Thickness Stress Predictions for Advanced Composite Material Configurations"

- Invited Paper to be Presented

SECTAM XII, Callaway Gardens, Georgia, May 9-11, 1983

"A Higher Order Displacement Formulation for Natural Vibration of Plates"

The schedule of work performance is presented below for the three year program. This schedule is as originally proposed as no changes are requested.

WORK SCHEDULE BY TASK

| TASK | YEAR 1 | | YEAR 2 | | YEAR 3 | | DOLLARS |
|----------|---------|------------|---------|------------|---------|------------|---------|
| | Dollars | % Complete | Dollars | % Complete | Dollars | % Complete | |
| TASK I | 35485 | 45 | 35485 | 90 | 7886 | 100 | 78856 |
| TASK II | 30468 | 25 | 31475 | 50 | 61973 | 100 | 123916 |
| TASK III | 2253 | 10 | 7567 | 44 | 12710 | 100 | 22530 |
| DOLLARS | 68206 | | 74527 | | 82569 | | 225302 |

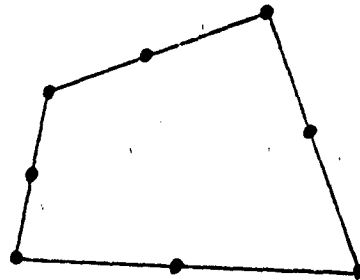
APPENDIX IA - HIGHER ORDER DISPLACEMENT MODELS

QHD40.

NODAL DEGREES OF FREEDOM:

Corner Nodes - $\{u_0 \ v_0 \ w_0 \ \psi_x \ \psi_y \ \phi_x \ \phi_y\}^T$

Mid-side Nodes - $\{w_0 \ \psi_x \ \psi_y\}^T$



DISPLACEMENT FIELD:

$$u = u_0 + z\psi_x + z^2\phi_x$$

$$v = v_0 + z\psi_y + z^2\phi_y$$

$$w = w_0$$

where;

$$u_0, v_0, \phi_x, \phi_y : \{1 \ x \ y \ xy\}^T \{\alpha\}$$

$$w_0, \psi_x, \psi_y : \{1 \ x \ y \ x^2 \ xy \ y^2 \ x^3y \ xy^3\}^T \{\beta\}$$

STRESS FIELD:

i. From constitutive relations - $\sigma_i = C_{ij}\epsilon_{ij}$ (orthotropic mat.)

$$\sigma_{xx} = f(z^2, x^2, y^2)$$

$$\sigma_{yy} = f(z^2, x^2, y^2)$$

$$\sigma_{xy} = f(z^2, x^2, y^2)$$

ii. From equilibrium considerations - $\sigma_{ij,j} = 0$

$$\sigma_{xz} = f(z^3, x, y)$$

$$\sigma_{yz} = f(z^3, x, y)$$

$$\sigma_{zz} = f(z^3)$$

QHD23

NODAL DEGREES OF FREEDOM:

$$\{u_0, v_0, w_0, \psi_x, \psi_y, \phi_x, \phi_y\}^T$$

DISPLACEMENT FIELD:

$$u = u_0 + z\psi_x + z^2\phi_x$$

$$v = v_0 + z\psi_y + z^2\phi_y$$

$$w = w_0$$

where;

$$u_0, v_0, w_0, \psi_x, \psi_y, \phi_x, \phi_y : \{1, x, y, xy\}^T(x)$$

STRESS FIELD:

i. From constitutive relations - $\sigma_{ij} = C_{ij}\epsilon_{ij}$ (orthotropic mat.)

$$\sigma_{xx} = f(z^2, x, y)$$

$$\sigma_{yy} = f(z^2, x, y)$$

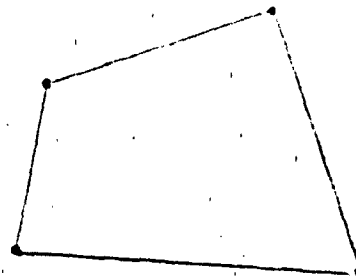
$$\sigma_{xy} = f(z^2, x, y)$$

ii. From constitutive considerations - $\sigma_{ij,j} = 0$

$$\sigma_{xz} = f(z^3)$$

$$\sigma_{yz} = f(z^3)$$

$$\sigma_{zz} = \text{constant}$$



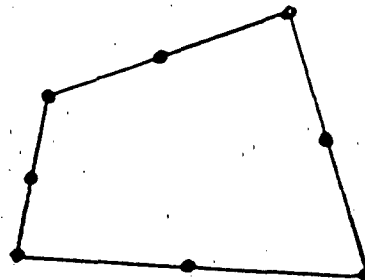
APPENDIX IB - MODIFIED KIRCHHOFF FORMULATION

QD32

NODAL DEGREES OF FREEDOM:

Corner Nodes $\{w_0 \ v_0 \ w \frac{\partial w}{\partial x} \frac{\partial w}{\partial y} \ \gamma_x \ \gamma_y\}^T$

Mid-Side Nodes $\{w \frac{\partial w}{\partial n}\}^T$



DISPLACEMENT FIELD:

$$w = f(x, y)$$

$$u = u_0 - z \left(\frac{\partial w}{\partial x} + \gamma_x \right)$$

$$v = v_0 - z \left(\frac{\partial w}{\partial y} + \gamma_y \right)$$

where:

$$u_0, v_0, \gamma_x, \gamma_y : \{1 \ x \ y \ xy\}^T \{4\}$$

$$w = \{1 \ x \ y \ x^2 \ xy \ y^2 \ x^3 \ x^2y \ xy^2 \ y^3 \ x^4 \ x^3y \ xy^3 \ y^4 \ x^4y \ xy^4\}^T \{3\}$$

STRESS FIELD:

i. From constitutive relations - $\sigma_i = C_{ij} \epsilon_{ij}$ (orthotropic mat.)

$$\sigma_{xx} = f(z, x^2, y^2)$$

$$\sigma_{yy} = f(z, x^2, y^2)$$

$$\sigma_{xy} = f(z, x^2, y^2)$$

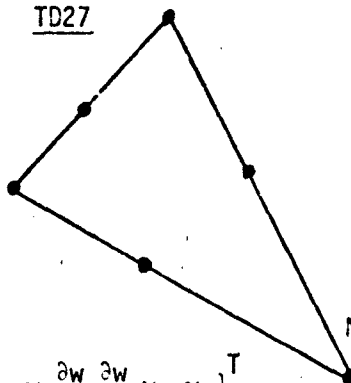
ii. From equilibrium considerations - $\sigma_{ij,i} = 0$

$$\sigma_{xz} = f(z^2, x^2, y^2)$$

$$\sigma_{yz} = f(z^2, x^2, y^2)$$

$$\sigma_{zz} = f(z^3, x, y)$$

TD27



$$\{u_0 \ v_0 \ w \ \frac{\partial w}{\partial x} \ \frac{\partial w}{\partial y} \ \gamma_x \ \gamma_y\}^T$$

$$\{w \ \frac{\partial w}{\partial n}\}^T$$

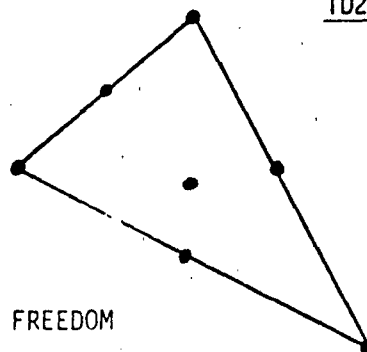
NODAL DEGREES OF FREEDOM

Corner Nodes

Mid-side Nodes

Center Node

TD27M



$$\{u_0 \ v_0 \ w \ \frac{\partial w}{\partial x} \ \frac{\partial w}{\partial y} \ \gamma_x \ \gamma_y\}^T$$

$$\{w\}^T$$

$$\{w \ \frac{\partial w}{\partial x} \ \frac{\partial w}{\partial y}\}^T$$

DISPLACEMENT FIELD

$$w = f(x, y)$$

$$u = u_0 - z \left(\frac{\partial w}{\partial x} + \gamma_x \right)$$

$$v = v_0 - z \left(\frac{\partial w}{\partial y} + \gamma_y \right)$$

where;

$$u_0, v_0, x, y : \{1 \ x \ y\}^T \{\alpha\}$$

$$w : \{1 \ x \ y \ x^2 \ xy \ y^2 \ x^3 \ x^2y \ xy^2 \ y^3 \ x^4 \ x^3y \ x^2y^2 \ xy^3 \ y^4\}^T \{\beta\}$$

STRESS FIELD

i. From constitutive relations $\sigma_i = C_{ij} \epsilon_{ij}$ (orthotropic mat.)

$$\sigma_{xx} = f(z, x^2, y^2)$$

$$\sigma_{yy} = f(z, x^2, y^2)$$

$$\sigma_{xy} = f(z, x^2, y^2)$$

ii. From equilibrium considerations $\sigma_{ij,ij} = 0$

$$\sigma_{xx} = f(z^3, x, y)$$

$$\sigma_{yz} = f(z^2, x, y)$$

$$\sigma_{zz} = f(z^3)$$

APPENDIX II - HYBRID-STRESS FORMULATION

Q1'S32

DISPLACEMENT FIELD:

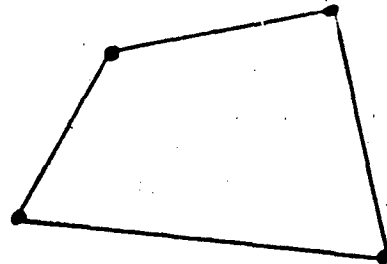
$$u = u_0 + z\psi_x + z^2\phi_x$$

$$v = v_0 + z\psi_y + z^2\phi_y$$

$$w = w_0 + z\phi_z$$

where;

$$u_0, v_0, \psi_x, \psi_y, \phi_z, \phi_x, \phi_y : \{1 \ x \ y \ xy\}^T \{\alpha\}$$



STRESS FIELD:

$$\sigma_x = (\beta_1 + \beta_2 x + \beta_3 y + \beta_4 xy) + z(\beta_5 + \beta_6 x + \beta_7 y + \beta_8 xy) + z^2(\beta_9 + \beta_{10} x + \beta_{11} y - \frac{3}{h^2} \beta_4 xy)$$

$$\sigma_y = (\beta_{12} + \beta_{13} x + \beta_{14} y - \beta_4 xy) + z(\beta_{15} + \beta_{16} x + \beta_{17} y + \beta_{18} xy) + z^2(\beta_{19} - \beta_{10} x - \beta_{11} y + \frac{3}{h^2} \beta_4 xy)$$

$$\sigma_{xy} = [\beta_{20} + (-\beta_{15} - \frac{h^2}{3} \beta_{21} + \frac{h^2}{3} \beta_{11})x + (-\beta_2 - \frac{h^2}{3} \beta_{10} - \frac{h^2}{3} \beta_{22})y + (-\beta_9 - \beta_{19})xy] + z[\beta_{23} + \beta_{24} x + \beta_{25} y + (-\frac{3}{h} \beta_9 - \frac{3}{h} \beta_{19})xy] + z^2[\beta_{26} + \beta_{21} x + \beta_{22} y + (\frac{3}{h^2} \beta_9 + \frac{3}{h^2} \beta_{19})xy]$$

$$\sigma_{xz} = (-h - z) [-\frac{h^2}{3} (\beta_{10} + \beta_{22}) + \beta_4 y + (-\beta_9 - \beta_{19})x] + \frac{1}{2}(h^2 - z^2) [\beta_6 + \beta_{25} + \beta_8 y - \frac{3}{h} (\beta_9 + \beta_{19})x] + \frac{1}{3}(-h^3 - z^3) [\beta_{10} - \frac{3}{h^2} \beta_4 y + \beta_{22} + \frac{3}{h^2} (\beta_9 + \beta_{19})x]$$

$$\sigma_{yz} = (-h - z) [-\frac{h^2}{3} \beta_{21} + \frac{h^2}{3} \beta_{11}] + (-\beta_9 - \beta_{19})y - \beta_4 x + \frac{1}{2}(h^2 - z^2) [\beta_{24} - \frac{3}{h} (\beta_9 + \beta_{19})y + \beta_{17} + \beta_{18} x] + \frac{1}{3}(-h^3 - z^3) [\beta_{21} + \frac{3}{h^2} (\beta_9 + \beta_{19})y - \beta_{11} + \frac{3}{h^2} \beta_4 x]$$

$$\sigma_z = (\beta_9 + \beta_{19}) [-(h + z)^2 - \frac{(-2h^3 - 3h^2 z + z^3)}{h}] + \frac{(3h^4 + 4h^3 z + z^4)}{2h^2}]$$

APPENDIX III - MASS MATRIX FORMULATION

The mass matrix for elements under development is easily arrived at by considering kinetic energy in the form

$$T = \frac{1}{2} \int_V \rho (\dot{u}^2 + \dot{v}^2 + \dot{w}^2) dV$$

where u , v and w represent displacements, ρ is the mass density, and the dot superscript denotes velocity. Defining velocities in terms of element shape functions gives

$$\dot{u} = \frac{1}{2} [\dot{L}] \int_V \rho \{N_U\} [N_U] + \{N_V\} [N_V] + \{N_W\} [N_W] dV \{\Delta\}$$

which is the classical form

$$T = \frac{1}{2} [\dot{A}] [M] \{\dot{A}\}$$

The element mass matrix $[M]$ is, therefore, specified as

$$[M] = \int_V \rho \{N_U\} [N_U] + \{N_V\} [N_V] + \{N_W\} [N_W] dV$$

Note that the shape functions $[N_i]$ involve distance from the mid-plane of the element to a layer denoted by Z and, therefore, the mass matrix definition provided not only represents mid-plane inertial effects but also rotary inertia as well.

APPENDIX IV - LARGE DISPLACEMENT FORMULATION

Based on Green's Strain Tensor, the following procedure is utilized to obtain the large displacement and the geometric stiffness matrices.

Let N be shape functions relating displacements at any point in the element $\{\delta\}$ to nodal displacements $\{\Delta\}$ such that

$$\{\delta\} = [N]\{\Delta\}$$

Also let $\{N_{i,j}\}^T$ denote those shape functions associated with the i^{th} displacement field ($i = u, v, w$) and " j " denotes the differentiation with respect to the j^{th} coordinate, i.e., $\frac{\partial}{\partial x_j}$ where $x_1 = x$, $x_2 = y$ and $x_3 = z$. Then, the strain ϵ_{xx} given by

$$\epsilon_{xx} = \frac{\partial u}{\partial x} + \frac{1}{2} \left[\left(\frac{\partial u}{\partial x} \right)^2 + \left(\frac{\partial v}{\partial x} \right)^2 + \left(\frac{\partial w}{\partial x} \right)^2 \right]$$

can be written as

$$\epsilon_{xx} = \{N_{u,x}\}^T \{\Delta\} + \frac{1}{2} \{\Delta\}^T \left\{ \{N_{u,x}\}^T \{N_{u,x}\} + \{N_{v,x}\}^T \{N_{v,x}\} + \{N_{w,x}\}^T \{N_{w,x}\} \right\} \{\Delta\}$$

Similarly; the shear strain ϵ_{xy} can be represented by

$$\begin{aligned} \epsilon_{xy} = & \left\{ \{N_{u,y}\}^T + \{N_{v,x}\}^T \right\} \{\Delta\}^T + \{\Delta\}^T \left\{ \{N_{u,x}\}^T \{N_{u,y}\} + \{N_{v,x}\}^T \{N_{v,y}\} \right. \\ & \left. + \{N_{w,x}\}^T \{N_{w,y}\} \right\} \{\Delta\} \end{aligned}$$

The strain field in indicial notation is expressed by

$$\{\epsilon_{ij}\} = \frac{1}{2} \left\{ \left[\{N_{i,j}\}^T + \{N_{j,i}\}^T \right] \{\Delta\} + \{\Delta\}^T \left[\{N_{k,i}\}^T \{N_{k,j}\} \right] \{\Delta\} \right\}$$

Then the incremental representation becomes

$$\{\delta \epsilon_{ij}\} = \frac{1}{2} \left[\left\{ \{N_{i,j}\}^T + \{N_{j,i}\}^T \right\} \{\delta \Delta\} + \{\delta \Delta\}^T \left[\{N_{k,i}\}^T \{N_{k,j}\} \right] \{\Delta\} + \{\Delta\}^T \left[\{N_{k,i}\}^T \{N_{k,j}\} \right] \{\delta \Delta\} \right]$$

But the second term can be expressed as

$$\{\Delta\}^T \left[\{N_{k,j}\}^T \{N_{k,i}\} \right] \{\delta \Delta\}$$

Thus combining terms

$$\{\delta \epsilon_{ij}\} = \frac{1}{2} \left[\left\{ \{N_{i,j}\}^T + \{N_{j,i}\}^T \right\} \{\delta \Delta\} + \{\delta \Delta\}^T \left[\{N_{k,i}\}^T \{N_{k,j}\} + \{N_{k,j}\}^T \{N_{k,i}\} \right] \{\delta \Delta\} \right]$$

Let

$$[B_0] = \frac{1}{2} \left[\{N_{i,j}\}^T + \{N_{j,i}\}^T \right]$$

$$[B_L] = \frac{1}{2} \{\Delta\}^T \left[\{N_{k,i}\}^T \{N_{k,j}\} + \{N_{k,j}\}^T \{N_{k,i}\} \right] =$$

$$\begin{bmatrix} \{\Delta\}^T [M_{xx}] \\ \{\Delta\}^T [M_{yy}] \\ \{\Delta\}^T [M_{xy}] \\ \{\Delta\}^T [M_{zz}] \\ \{\Delta\}^T [M_{xz}] \\ \{\Delta\}^T [M_{yz}] \end{bmatrix}$$

Then

$$\{\delta \epsilon_{ij}\} = [B_0] \{\delta \Delta\} + [B_L] \{\delta \Delta\}$$

where $[B_0]$ is the linear component and $[B_L]$ is the large displacement component. Having the definitions for $[B_0]$ and $[B_L]$, the small and large displacement matrices $[K_0]$ and $[K_L]$ are represented as

$$[K_0] = \int_V [B_0]^T [D] [B_0] dV$$

$$[K_L] = \int_V \left\{ [B_L]^T [D] [B_0] + [B_L]^T [D] [B_L] + [B_0]^T [D] [B_L] \right\} dV$$

The geometric stiffness matrix is also derived from $[B_L]$ and it has the following form

$$[KG] = \int_V \left(\sigma_{xx}[M_{xx}] + \sigma_{yy}[M_{yy}] + \sigma_{zz}[M_{zz}] + \sigma_{xy}[M_{xy}] + \sigma_{xz}[M_{xz}] + \sigma_{yz}[M_{yz}] \right) dV$$

Where the σ 's are the stress components and again integration is on a layer by layer basis.